The human visual cortex response to melanopsin-directed stimulation is accompanied by a distinct perceptual experience

Manuel Spitschan[a], Andrew S. Bock[b], Jack Ryan[b], Giulia Frazzetta[b], David H. Brainard[a], and Geoffrey K. Aguirre[b,1]

[a]Department of Psychology, University of Pennsylvania, Philadelphia, PA 19104; and [b]Department of Neurology, Perelman School of Medicine, University of Pennsylvania, Philadelphia, PA 19104

Edited by Brian A. Wandell, Stanford University, Stanford, CA, and approved September 28, 2017 (received for review June 27, 2017)

The photopigment melanopsin supports reflexive visual functions in people, such as pupil constriction and circadian photoentrainment. What contribution melanopsin makes to conscious visual perception is less studied. We devised a stimulus that targeted melanopsin separately from the cones using pulsed (3-s) spectral modulations around a photopic background. Pupillometry confirmed that the melanopsin stimulus evokes a response different from that produced by cone stimulation. In each of four subjects, a functional MRI response in area V1 was found. This response scaled with melanopic contrast and was not easily explained by imprecision in the silencing of the cones. Twenty additional subjects then observed melanopsin pulses and provided a structured rating of the perceptual experience. Melanopsin stimulation was described as an unpleasant, blurry, minimal brightening that quickly faded. We conclude that isolated stimulation of melanopsin is likely associated with a response within the cortical visual pathway and with an evoked conscious percept.

melanopsin | ipRGCs | vision | visual cortex | fMRI

Human visual perception under daylight conditions is well described by the combination of signals from the short (S)-, medium (M)-, and long (L)-wavelength cones (1). Melanopsin-containing intrinsically photosensitive retinal ganglion cells (ipRGCs) are also active in bright light (Fig. 1*A*). The ipRGCs have notably prolonged responses to changes in light level and thus signal retinal irradiance in their tonic firing (2). Studies in rodents, nonhuman primates, and people have emphasized the role of the ipRGCs in reflexive, nonimage-forming visual functions that integrate information over tens of seconds to hours, such as circadian photoentrainment, pupil control, and somatosensory discomfort from bright light (3–6).

Relatively unexamined is the effect of melanopsin phototransduction upon visual perception, which operates at shorter timescales (7–9). In addition to tonic firing, ipRGCs exhibit transient responses to flashes of light with an onset latency as short as 200 ms (10). Several ipRGC subtypes project to the lateral geniculate nucleus, where they are found to drive both transient and tonic neural responses (2, 11–13). As the geniculate is the starting point of the cortical pathway for visual perception, it is possible that ipRGC activity has a conscious visual perceptual correlate.

Here we examine whether melanopsin-directed stimulation drives responses within human visual cortex and characterize the associated perceptual experience. Our approach uses tailored modulations of the spectral content of a light stimulus, allowing melanopsin to be targeted separately from the cones in visually normal subjects (14, 15). We also studied the converse modulation, which drives the cone-based luminance channel while minimizing melanopsin stimulation. We collected blood oxygenation level-dependent (BOLD) functional magnetic resonance imaging (fMRI) data while subjects viewed brief (3-s) pulses of these spectral modulations. Concurrent infrared pupillometry was used to confirm that our stimuli elicit responses from distinct retinal mechanisms. Finally, we characterized the perceptual experience of selective melanopsin-directed stimulation and examined whether this experience is distinct from that caused by stimulation of the cones.

Results

Four subjects were studied in multiple experiments while they viewed intermittent pulses of spectral contrast directed at either the postreceptoral luminance pathway (equal contrast on L, M, and S cones; LMS) or the melanopsin-containing ipRGCs (Fig. 1*A*). Different stimuli produced contrast upon the targeted photoreceptors between 25% and 400% (Fig. 1*B*; additional stimulus details in *SI Appendix*, Fig. S1). During fMRI scanning, subjects viewed these stimuli with their pharmacologically dilated right eye; in some experiments the consensual response of the left pupil was also recorded with an infrared camera (Fig. 1*C*). On each of many trials a 3-s spectral pulse was presented (Fig. 1*D*). The subject maintained fixation upon a masked central disk (Fig. 1*E*), while spectral changes occurred in the visual periphery. The stimulus and background spectra had a light-orange hue as they had relatively less power at short wavelengths.

V1 Cortex Responds to Melanopsin Contrast. We first examined the extent of cortical response to high-contrast spectral pulses. Each subject viewed 200 pulses each of the 400% luminance and

Significance

Melanopsin-containing retinal cells detect bright light and contribute to reflex visual responses such as pupil constriction. Their role in conscious, cortical vision is less understood. Using functional MRI to measure brain activity, we find that melanopsin-directed stimulation reaches the visual cortex in people. Such stimulation also produces a distinct perceptual experience. Our results have clinical importance as melanopsin function may contribute to the discomfort that some people experience from bright light.

Author contributions: M.S., D.H.B., and G.K.A. conceived the project; M.S. and G.K.A. designed the fMRI experiments; J.R., D.H.B., and G.K.A. designed the perceptual experiment; M.S. and D.H.B. designed the spectral modulations; M.S., A.S.B., J.R., G.F., and G.K.A. collected fMRI data; G.F. collected pupillometry data; J.R. collected perceptual data; M.S., A.S.B., and G.F. analyzed fMRI data; M.S. and G.F. analyzed pupillometry data; G.K.A. implemented temporal models for the fMRI and pupillometry data; J.R., D.H.B., and G.K.A. analyzed perceptual data; M.S. analyzed the effects of biological variability upon photoreceptor contrast; G.K.A. created the figures; and M.S. and G.K.A. wrote the paper with contributions from A.S.B., J.R., G.F., and D.H.B.

Conflict of interest statement: G.K.A., D.H.B., and M.S. are listed as inventors on a patent application filed by the Trustees of the University of Pennsylvania on September 11, 2015 (US Patent Application No. 14/852,001, "Robust Targeting of Photosensitive Molecules"). The authors declare no other competing financial interests.

This article is a PNAS Direct Submission.

[1]To whom correspondence should be addressed. Email: aguirreg@upenn.edu.

This article contains supporting information online at www.pnas.org/lookup/suppl/doi:10.1073/pnas.1711522114/-/DCSupplemental.

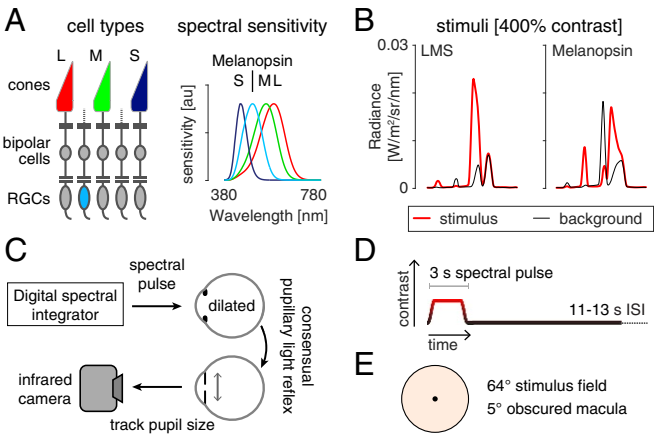

Fig. 1. Overview and experimental design. (*A*, *Left*) The L, M, and S cones, and melanopsin-containing ipRGCs, mediate visual function at daytime light levels. (*A*, *Right*) The spectral sensitivities of these photoreceptor classes. (*B*) Stimulus spectra. Changes between a background (black) and stimulus (red) spectra targeted a given photoreceptor channel. The 400% contrast stimuli are shown. (*B*, *Left*) Spectra targeting the L, M, and S cones and thus the postreceptoral luminance channel. The nominal melanopic contrast for this modulation was zero. (*B*, *Right*) The corresponding spectra for stimuli targeting melanopsin. The nominal L-, M-, and S-cone contrast of this stimulus was zero. (*C*) During fMRI scanning, subjects viewed pulsed spectral modulations, produced by a digital spectral integrator, with their pharmacologically dilated right eye. The consensual pupil response of the left eye was recorded in some experiments. (*D*) Multiple 3-s, pulsed spectral modulations were presented, windowed by a 500-ms half-cosine at onset and offset, and followed by an 11- to 13-s interstimulus interval (ISI). A given experiment presented either a single contrast level, or multiple contrast levels in a counterbalanced order. (*E*) Spectra were presented on a uniform field of 64° (visual angle) diameter. Subjects fixated the center of a 5° masked region, minimizing macular stimulation. The stimulus spectra had a light-orange hue.

melanopsin stimuli. We measured the reliability of the evoked response within subject and then at a second level across subjects and the two hemispheres. Pulses of luminance contrast that minimized melanopsin stimulation (Fig. 2*A*) produced responses in the early cortical visual areas, generally corresponding to the retinotopic projection of the stimulated portion of the visual field (16). Spectral pulses directed at melanopsin that minimized cone stimulation also evoked responses within the visual cortex (Fig. 2*B*). In subsequent experiments, we examined the evoked responses to luminance and melanopsin stimulation within a region of interest in V1 cortex that lies entirely within the retinotopic projection of the stimulated visual field. The time-series data and evoked responses from within this region for the initial, 400% contrast only experiment can be found in *SI Appendix*, Fig. S2.

If the visual cortex encodes information from the ipRGCs, we would expect that the BOLD fMRI response should reflect the degree of melanopsin stimulation. Each of the four observers was studied again, this time with spectral pulses that varied in the degree of contrast upon the LMS or melanopsin channels. Fig. 2*C* shows an example of the data obtained from the V1 region of interest in response to luminance pulses during one scan run for one observer. The time series was fitted with a Fourier basis set that estimated the shape of the BOLD fMRI response evoked by stimuli of each contrast level. Fig. 2*D* presents the time-series data and evoked responses for the four subjects during luminance stimulation. Luminance pulses evoked consistent responses in the V1 region of interest, with a steadily increasing amplitude of evoked response across contrast levels. Variation in melanopic contrast (Fig. 2*E*) produced similar data, with an increasing amplitude of BOLD fMRI response to larger contrasts.

We fitted the evoked responses at each contrast level for each subject, using an empirical measure of the subject's hemodynamic response function, along with parameters that controlled the duration of an underlying neural response and the amplitude of the evoked BOLD fMRI signal (*SI Appendix*, Fig. S3). We obtained the amplitude of response as a function of contrast for each subject and each stimulus (Fig. 3; LMS and melanopsin; gray and blue lines, respectively). The measured amplitude increased as a function of contrast for both luminance and melanopsin stimulation for all four observers. While we modeled the duration of underlying neural activity, the results did not support the claim of a distinct temporal response to melanopsin stimulation (*SI Appendix*, Fig. S4).

While the melanopsin-directed spectral pulses were designed to produce no differential stimulation of the cones, biological variation and inevitable imperfection in device control result in some degree of unwanted cone stimulation (termed "splatter") (14, 15, 17). We considered the possibility that the visual cortex response to the melanopsin stimulus was in fact a response to a small amount of cone contrast inadvertently produced by our nominally cone-silent spectral pulses.

We obtained spectroradiometric measurements of the stimuli that were actually produced by our device at the time of the BOLD fMRI experiment for each subject. For each of these measurements we calculated the inadvertent contrast that the cones would have experienced within these 400% melanopsin modulations in a biologically typical subject. We took the maximum contrast values calculated for the measurements across subjects and created a new spectral pulse that was designed to have no melanopsin stimulation, but to have cone contrast equal to this estimate of inadvertent contrast. Scaled versions of this modulation corresponded to logarithmically spaced larger (2×) and smaller ($\frac{1}{2}\times$, $\frac{1}{4}\times$) multiples of the splatter contrast. We measured the amplitude of BOLD fMRI response as a function of splatter contrast (Fig. 3, green line). In all four subjects, the melanopsin response function was larger than the splatter response function. This indicates that the cortical response to melanopsin cannot be explained entirely by imperfection in stimulus generation. An additional analysis (*SI Appendix*, Fig. S5) indicates that it is unlikely that our results are explained by biological variation (18) in the modeled properties of the lens and retina used to calculate cone contrast.

Additional control experiments considered the possible influence of rod signals or eye movements and are described in *SI Appendix*, Figs S6 and S7).

Different Kinetics of Pupil Response to Melanopic and Luminance Pulses. We recorded pupil responses during the presentation of melanopsin and LMS stimuli of varying contrast. We tested whether the responses to the two stimulus types differ, as such a demonstration would increase confidence that our stimuli target distinct retinal mechanisms.

The average pupil response was obtained for each contrast level and stimulus type. In the across-subject averages (Fig. 4*A*; individual subject data in *SI Appendix*, Fig. S8), an evoked response to LMS stimulation is seen at even the lowest contrast level (25%). As LMS contrast grows, the evoked pupil response becomes larger, with distinct features corresponding to the onset and the offset of the 3-s stimulus pulse. The response to melanopsin contrast (Fig. 4*B*) begins smaller, but also increases with contrast. Unlike the pupil response to LMS contrast, it is difficult to discern the point of stimulus offset in the extended response to melanopsin stimulation.

We quantified these observations by fitting a temporal model (*SI Appendix*, Fig. S9) to the average evoked pupil responses. The model has three temporally distinct components that capture an initial transient constriction of the pupil at stimulus onset,

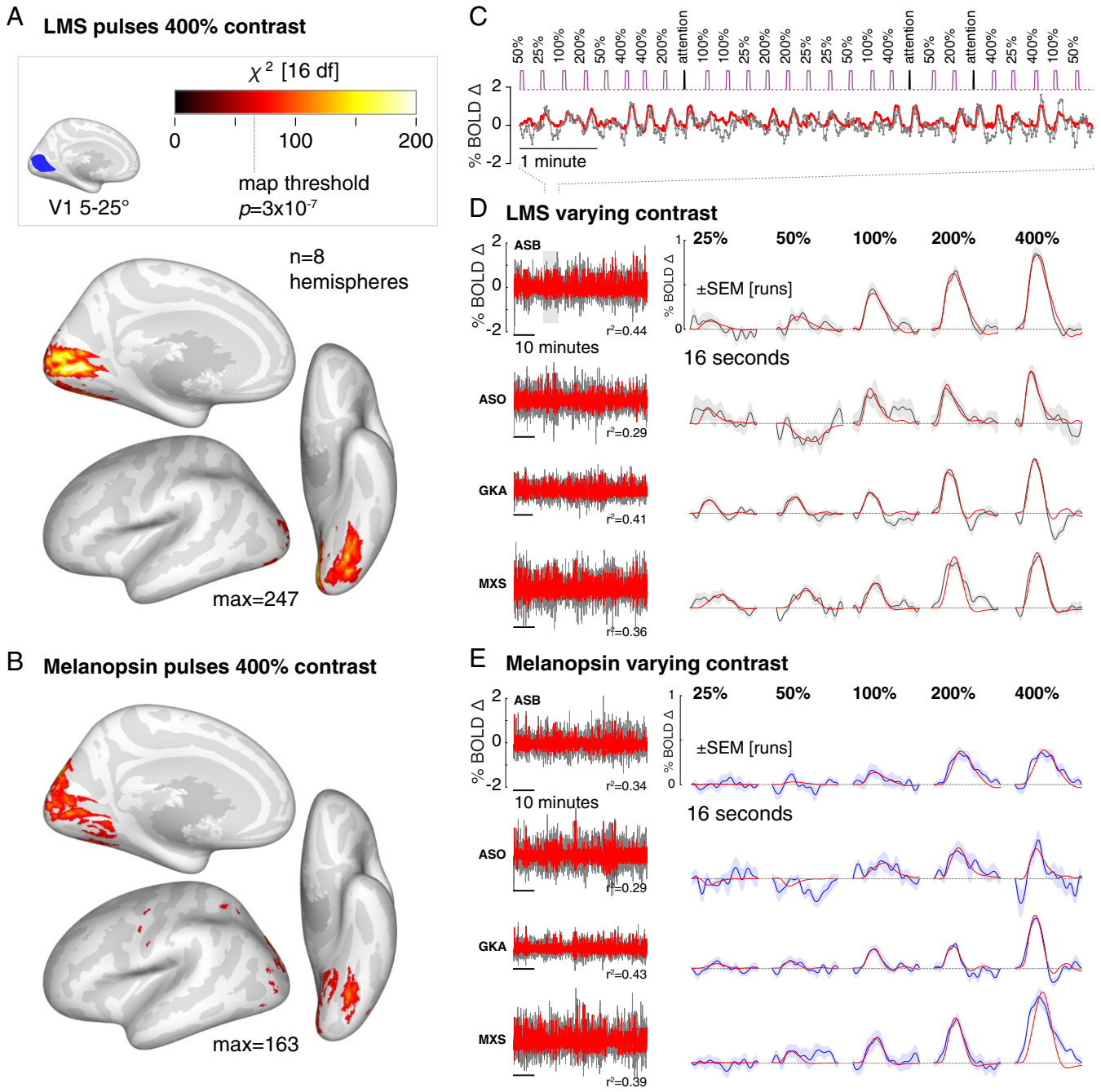

Fig. 2. Visual cortex responses to LMS and melanopsin contrast. (*A*) Cortical response to pulses of 400% LMS contrast across subjects and hemispheres. Threshold corresponds to a map-wise $\alpha = 0.05$ (Bonferroni corrected for the number of vertices). *A*, *Inset* shows the region of V1 cortex with retinotopic representation corresponding to the visual field range of 5–25° radial eccentricity, indicated in blue. Subsequent analyses examine the mean signal from this region. (*B*) The corresponding surface map obtained in response to 400% melanopsin contrast pulses. (*C*) Example fit (red) of the Fourier basis set to a portion of the BOLD fMRI time-series data (gray). (*D*) V1 responses to LMS stimulation of varying contrast. (*D*, *Left*) The BOLD fMRI time-series data from the area V1 region for each subject (black), following preprocessing to remove nuisance effects. A Fourier basis set modeled (red) the mean evoked response to each contrast level with the r^2 value of the model fit indicated. (*D*, *Right*) The evoked responses for each subject and stimulus level (black) and SEM of the response across the 9–11 scanning runs performed in each subject (shaded region). The responses were fitted by a model (red) that convolved a step function of neural activity by the hemodynamic response function measured for each subject (*SI Appendix*, Fig. S3). (*E*) The corresponding responses within the V1 region to melanopsin stimulation of varying contrast.

a sustained response that tracks the stimulus profile, and a persistent response as the pupil slowly redilates (Fig. 4 *A* and *B*, *Insets* and *C*, *Left*, *Inset*). The amplitude of each of these components was measured as a function of contrast for the LMS and melanopsin stimuli (Fig. 4*C*; temporal parameter values in *SI Appendix*, Fig. S10). The amplitude of both the initial transient and persistent response increase with LMS and melanopsin contrast. The behavior of the sustained component, however, is different for the two types of stimulation. Luminance contrast produces steadily increasing sustained pupil constriction that is time locked to the profile of the stimulus. In contrast, there is essentially no component of this kind in the melanopsin-driven

pupil response. This behavior is in keeping with the temporally low-pass properties of the melanopsin system (15).

Melanopsin Stimulation Evokes a Distinct Visual Percept. We examined the perceptual experience produced by our stimuli. Twenty subjects viewed 400% contrast pulses of LMS, melanopsin, and a third stimulus that changed in power by an equal multiplicative factor across all wavelengths, thus stimulating both melanopsin and luminance channels ("light flux"). Subjects rated nine perceptual qualities of the light pulse, each quality defined by a pair of antonyms (e.g., dim to bright). Subjects were not informed of the different identities of the stimuli, and the order was randomized as described in *SI Appendix*, *SI Text Online Methods*. Subjects were also invited to offer their free-form observations during a debriefing session (summarized in *SI Appendix*, Table S2). We implemented additional stimulus calibration measures to further reduce spectral variation due to device instability (*SI Appendix*, Fig. S11).

Subjects rated each property of each stimulus twice, allowing us to confirm that within-subject reliability was high (across-subject mean Spearman correlation of test–retest reliability = 0.73 ± 0.18 SD). Additionally, there was good subject agreement in the ratings (across-subject mean Spearman correlation of ratings from one left-out subject to mean ratings of all other subjects = 0.53 ± 0.13 SD).

Subjects consistently rated the melanopsin stimulus as perceptually distinct from the LMS or light flux pulses (*SI Appendix*, Table S1). We summarized these measurements by submitting them to a principal components analysis (Fig. 5*A*). The first and second dimensions explained 35% and 19% of the variance in ratings, respectively. Within this space a support vector machine could classify subject responses to melanopsin as distinct from those for LMS or light flux with 92% cross-validated accuracy. A plot of the weights that define the classification dimension (Fig. 5*B*) reveals the primary qualities of melanopsin stimulation. To these subjects, and in our own experience, the onset of the melanopsin contrast appears as a somewhat unpleasant, blurry, minimal brightening of the field. Most notably, however, this percept is fleeting and rapidly followed by a fading or loss of perception from the stimulus field. Many of the subjects described the melanopsin stimulus pulse as being colored. This was typically a yellow–orange appearance, although three subjects reported a greenish percept.

The perceptual ratings of the LMS and light flux stimuli were quite similar, with the LMS rated as having more color (again perhaps due to the inadvertent chromatic contrast present in the stimulus; *SI Appendix*, Fig. S11) and the light flux as being brighter. Prior studies have found that melanopsin contrast is additive to LMS contrast in the perception of brightness (7). In our data, this would be consistent with higher ratings on the dim-to-bright scale for light flux pulses compared with LMS. A post hoc test supported this interpretation (Wilcoxon signed-rank test of dim-to-bright ratings in light flux compared with LMS: $P = 0.0088$).

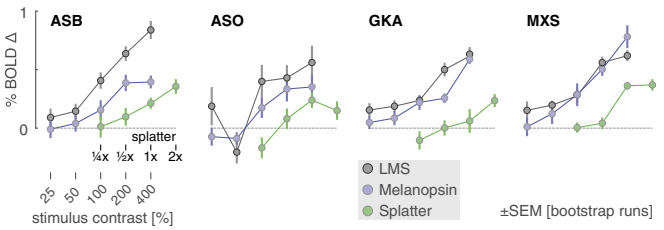

Fig. 3. V1 BOLD fMRI response by stimulus contrast. The amplitude of evoked response within the V1 region was obtained for each subject and contrast level for the luminance (gray), melanopsin (cyan), and splatter (green) stimulus conditions. The 1× splatter condition presented cone contrast equal to the maximal inadvertent contrast (resulting from imperfections in device control) estimated from measurements of the spectra in the melanopsin experiments.

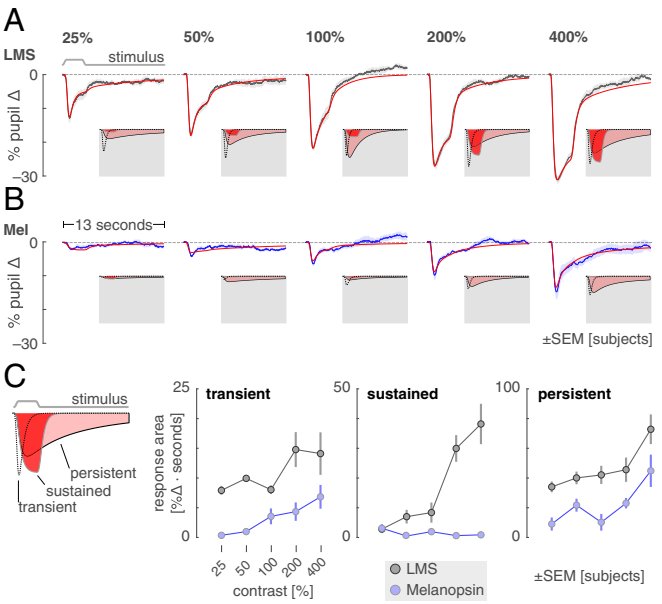

Fig. 4. Consensual pupil responses to LMS and melanopsin stimulation. The consensual pupil response of the left eye was measured during stimulation of the pharmacologically dilated right eye. (*A*) The mean (across subjects) pupil response evoked by LMS stimulation of varying contrast levels (black), with SEM across subjects (shaded). The evoked response was fitted with a three-component, six-parameter model (red). *Insets* on a gray field show the three components that model each response. (*B*) The corresponding mean pupil responses evoked by melanopsin stimulation of varying contrast levels. (*C*) Amplitude of the three model components as a function of stimulus contrast. *C*, *Inset* (*Left*) is an illustration of the three model components. *C*, *Right* shows the gain parameter for each model component as a function of contrast for LMS (gray) and melanopsin (blue) stimulation.

Discussion

Our studies indicate a role for the melanopsin-containing ipRGCs in conscious human vision. We find that high-contrast spectral exchanges designed to isolate melanopsin evoke responses in human visual cortex. Pupil responses to these stimuli are distinct from those produced by luminance contrast, consistent with separation of retinal mechanisms. The cortical response is not easily explained by inadvertent stimulation of the cones and is associated with a distinct perceptual experience.

Previous studies in rodents and humans with outer photoreceptor defects have suggested that the visual cortex responds to melanopsin stimulation. Zaidi et al. (19) reported the case of an 87-y-old woman with autosomal-dominant cone–rod dystrophy who was able to correctly report the presence of an intense, 480-nm 10-s light pulse, but not other wavelengths. Similarly, in mice lacking rods and cones, the presentation of a narrowband 447-nm light evoked a hemodynamic (optical imaging) signal change in the rodent visual cortex, with a slightly delayed onset (1 s) and a reduced amplitude compared with the same measurement in a wild-type mouse (11). In our work we measured cortical and perceptual responses to melanopsin-directed stimulation in the intact human visual system.

A Cortical Response. The melanopsin-containing ipRGCs have broad projections to subcortical sites (20). Studies in the rodent and primate demonstrate as well projections to the lateral geniculate nucleus, where evoked responses to melanopsin

stimulation can be found (2, 11–13). Whether these signals are further transmitted to the visual cortex in normally sighted humans or nonhuman animals has been unknown. We find that pulsed melanopsin stimulation evokes contrast-graded responses within primary visual cortex. Responses to the highest (400%) contrast stimulus extend into adjacent, retinotopically organized visual areas, including ventrally in the vicinity of the peripheral representation for hV4 and VO1 (21); a similar spatial distribution of cortical responses was observed to luminance stimulation.

By using a background with reduced short-wavelength light (8), we created substantial melanopic contrast in our stimuli, albeit ∼3.5× less than is available in rodent models with a shifted long-wavelength cone. (12) We found that 100% contrast pulses were required to obtain a measurable cortical response to melanopsin. The contrast response functions for both V1 fMRI amplitude and persistent pupil constriction appeared to be in the linear range and rising even at our maximum, 400% contrast level.

A Visual Percept. Consistent with the presence of a V1 neural response, we find that melanopsin-directed stimulation is accompanied by a distinct visual percept. We viewed these stimuli over many hours of experiments and ourselves experienced the onset of the melanopsin spectral pulse as a diffuse, minimal brightening of the visual field. The appearance was curiously unpleasant.

The diffuse, even blurry, property of the percept might be related to the broad receptive fields of neurons driven by melanopsin stimulation (22), consistent with the extensive dendritic arbors of the ipRGCs (23). In a prior study, subjects reported that lights appear brighter when melanopsin contrast is added to the stimulation of the cone-based luminance channel (7). We find a conceptually similar effect in our data, as subjects rated pulses of light flux (which contain melanopic contrast) as brighter than pulses with cone contrast alone.

The most striking aspect of the percept evoked by the melanopsin pulse is that the brief brightening is then followed by a fading of perception of the stimulus field, on occasion spreading to involve the masked macular region of the stimulus. This was subjectively similar to Troxler fading. This aspect was remarked upon by several of our observers: "[the experience was] like blinding," and "[the fade] to black that is the noise when your eyes are closed" or "kind of like if you got hit in the head really sharply … flashing lights and fade out." (*SI Appendix*, Table S2). The melanopsin-containing ipRGCs send recurrent axon collaterals to the inner plexiform layer where they are positioned to modulate cone signals (24). Consistent with this, melanopic contrast has been shown to attenuate cone-driven electroretinogram responses in the rodent over minutes (12). The prominent and rapid experience of fading for our melanopsin-directed stimulus perhaps reflects the unopposed action of this attenuation mechanism.

Our data do not allow us to determine whether one or more of the reported perceptual experiences arising from melanopsin stimulation are a direct consequence of ipRGC signals arriving at visual cortex sites or from the interaction of melanopsin and cone signals at earlier points in the visual pathway.

The Challenge of Photoreceptor Isolation. Our conclusions depend upon the successful isolation of targeted photoreceptor channels. Measurements and simulations indicate that the fMRI results are unlikely to be explained by inadvertent cone contrast from known sources of biological variation (*SI Appendix*, Fig. S5) (18). Nonetheless, we think it prudent to carry forward concern regarding inadvertent cone intrusion and to search for additional means to exclude this possible influence. For example, in the present study we examined in the fMRI data whether there was a difference in the time course of response to luminance and melanopsin-directed stimuli, but did not find convincing evidence of such (*SI Appendix*, Fig. S3). A time-course dissociation in the fMRI data would have provided further support—similar to that obtained in the pupil data—that our stimuli drive distinct mechanisms. Different temporal profiles of stimulation may afford greater traction on this question in future studies.

In our perceptual experiment, the melanopsin stimulus was reported to have a change in hue. This was usually, but not universally, reported as yellow–orange. In this experiment we do not have available an estimate of the amount of reported color change that may be attributable to imperfections in cone silencing. Consequently, we are unable to reject the possibility that small amounts of chromatic splatter produce this percept.

Our results are also subject to any systematic deviation of photoreceptor sensitivity from that assumed in the design of our spectral modulations. One example model deviation is the presence of "penumbral" cones that lie in the shadow of blood vessels and thus receive the stimulus spectrum after it has passed through the hemoglobin transmittance function. These photoreceptors can be inadvertently stimulated by a melanopsin-directed modulation, producing a percept of the retinal blood vessels when the spectra are rapidly flickered (≥4 Hz) (17). While it is possible to also silence the penumbral cones in the melanopsin stimulus (14), this markedly reduces available contrast upon melanopsin (below 100%). We circumvented this problem here by windowing the onset of the melanopsin stimulus with a gradual transition (effectively 1 Hz) that removed the penumbral cone percept from our stimulus pulse.

We note that these challenges attend our prior study of cortical responses to rapid melanopsin flicker (14). In those experiments, penumbral-cone silent, sinusoidal melanopsin modulations with 16% Michelson contrast were studied. For comparison with the stimuli used in the present study, we can express contrast as the peak of the sinusoid relative to the trough. This yields ∼40% Weber contrast. Given our finding here that roughly 100% Weber contrast was needed to evoke a V1 response, we now regard our prior study as not fully resolving the possibility that rapid modulation of the ipRGCs drives a cortical response.

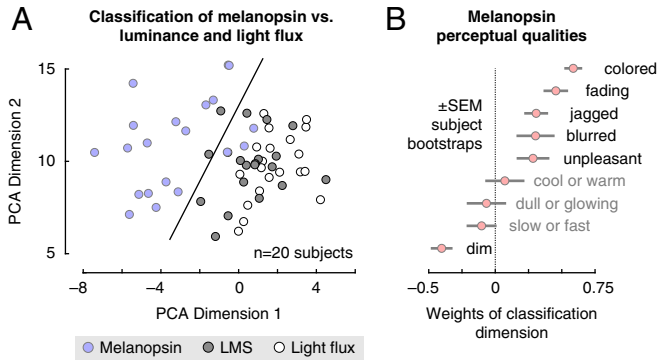

Fig. 5. Perceptual ratings of melanopsin, luminance, and light flux. Subjects rated nine qualities of spectral pulses that targeted melanopsin, luminance, and their combination (light flux). (*A*) The set of perceptual ratings was subjected to a principal components analysis. Each circle corresponds to the ratings provided by one subject for one stimulus type within the space defined by the first two dimensions of the PCA solution. A linear support-vector machine was trained to distinguish ratings for melanopsin stimulation from the other two stimulus types within this 2D space. The classification boundary is shown. (*B*) The classification dimension (normal to the classification boundary) describes how melanopsin stimulation was perceived differently from light flux and luminance. The mean weights (across bootstrap resamples) that define the classification dimension are shown.

The finding that melanopsin contributes to visual perception at photopic light levels in people challenges the orthodoxy that only three photopigments contribute to daylight vision. Two previous studies using silent substitution methodology reported psychophysical sensitivity in detection of cone-silent spectral modulations at photopic light levels (8, 9). These studies also faced the challenge of photoreceptor isolation, as even small imperfections in the silencing of cones could lead to detection. An inferential strength of the current study is that we measure a graded, suprathreshold visual cortex response to varying contrast levels, which we may compare with the effect of imprecision in cone silencing. Suprathreshold contrast also allowed us to characterize the appearance of the stimulus.

Conclusions

Our results suggest that people can "see" with melanopsin. The high-contrast, melanopsin-directed spectral modulation we studied is a distinctly unnatural stimulus but a valuable tool for demonstrating the presence of a melanopic signal in the cortical visual pathway. Many of our subjects found the melanopsin-directed stimulus to be unpleasant to view. We are curious whether variation in the perceptual or cortical response to this stimulus is related to the symptom of photophobia (6). Under naturalistic conditions, it appears that melanopsin adjusts the sensitivity of the cone pathways (12). The interaction of melanopsin and cone signals in human vision is an exciting avenue for investigation, particularly given recent findings of a role for melanopsin in the coarse spatial coding of light intensity (22).

Materials and Methods

A digital light synthesis engine (OneLight Spectra) was used to produce spectral modulations that targeted either the melanopsin photopigment or the LMS cones with varying contrast (25%, 50%, 100%, 200%, and 400%) against a rod-saturating background [100–200 candelas/m^2 (cd/m^2); $>$3.3 $\log_{10}$ scotopic trolands (sc td)]. Pulse stimuli (3 s, cosine windowed at onset and offset) were presented within a wide-field, uniform annulus with an outer diameter of 64° and an inner diameter of 5°, minimizing macular stimulation. Stimuli were adjusted for each observer's nominal age to account for age-specific prereceptoral filtering (*SI Appendix, SI Text Online Methods*). The quality of photopigment isolation was assessed by combining spectroradiometric measurements of the stimuli with a resampling approach that modeled sources of biological variation in photoreceptor spectral sensitivity (*SI Appendix, SI Text Online Methods*).

Four observers (four men, aged 27 y, 28 y, 32 y, and 46 y, three of whom are authors of this study) viewed the stimuli with their pharmacologically dilated right eye while they underwent fMRI scanning. The consensual pupillary response to the stimuli was measured from the left eye during some scanning sessions, using an infrared eye tracker. Stimulus pulses were jittered in their onset timing and spaced 14–16 s apart. Subjects were asked to detect an occasional, brief (500 ms) dimming of the stimulus field to which they made a button press. This served to monitor subject alertness and provided events that were used to derive a hemodynamic response function (HRF) for each observer.

BOLD fMRI data underwent standard preprocessing and were projected to a spherical atlas of cortical surface topology, supporting anatomical definition of the location and organization of retinotopic cortex (*SI Appendix, SI Text Online Methods*). Because stimuli were presented asynchronously with respect to fMRI acquisitions, the time-series data were fitted with a Fourier basis set to extract the average evoked response to each stimulus type. The resulting evoked response per stimulus type was then fitted with a two-parameter model incorporating the duration of an underlying step of neural activity and the amplitude of this response after convolution by the subject-specific HRF (*SI Appendix, SI Text Online Methods*).

In a separate experiment, conducted outside of the scanner, 20 observers (9 men, 11 women; mean age 27 y, range 20–33 y) viewed the LMS and melanopsin-directed stimuli, as well as pulses of broadband spectral change (light flux) which stimulated both cones and melanopsin. These observers were not involved in the design and conduct of the study and were not informed of the identity of the pulses. They were asked to rate the stimuli along nine perceptual dimensions, given as antonym pairs (*SI Appendix, SI Text Online Methods*).

This research was approved by the University of Pennsylvania Institutional Review Board and conducted in accordance with the principles of the Declaration of Helsinki. All subjects gave written informed consent. All experiments were preregistered in the Open Science Framework. All data and code are available. All raw data are available as packaged and MD5-hashed archives as well as tables detailing the biological variability on FigShare (https://figshare.com/s/0baea6ed50758abbabf4). All code is available in public GitHub repositories (https://github.com/gkaguirrelab/Spitschan_2017_PNAS/). Unthresholded statistical maps from experiments 1 and 2 for each subject are available from NeuroVault (https://neurovault.org/collections/2459/).

Detailed methods are described in *SI Appendix, SI Text Online Methods*.

ACKNOWLEDGMENTS. We thank Fred Letterio for technical assistance and Andrew S. Olsen for his assistance with data collection. This work was supported by National Institutes of Health Grant R01 EY024681 (to G.K.A. and D.H.B.), Core Grant for Vision Research P30 EY001583, Neuroscience Neuroimaging Center Core Grant P30 NS045839, and Department of Defense Grant W81XWH-15-1-0447 (to G.K.A.).

1. Stockman A, Brainard DH (2010) Color vision mechanisms. *The OSA Handbook of Optics*, ed Bass M (McGraw-Hill, New York), 3rd Ed, pp 11.1–11.104.
2. Dacey DM, et al. (2005) Melanopsin-expressing ganglion cells in primate retina signal colour and irradiance and project to the LGN. *Nature* 433:749–754.
3. Lucas RJ, et al. (2003) Diminished pupillary light reflex at high irradiances in melanopsin-knockout mice. *Science* 299:245–247.
4. Gamlin PDR, et al. (2007) Human and macaque pupil responses driven by melanopsin-containing retinal ganglion cells. *Vis Res* 47:946–954.
5. Hattar S, et al. (2003) Melanopsin and rod-cone photoreceptive systems account for all major accessory visual functions in mice. *Nature* 424:76–81.
6. Noseda R, et al. (2010) A neural mechanism for exacerbation of headache by light. *Nat Neurosci* 13:239–245.
7. Brown TM, et al. (2012) Melanopsin-based brightness discrimination in mice and humans. *Curr Biol* 22:1134–1141.
8. Cao D, Nicandro N, Barrionuevo PA (2015) A five-primary photostimulator suitable for studying intrinsically photosensitive retinal ganglion cell functions in humans. *J Vis* 15:27.
9. Horiguchi H, Winawer J, Dougherty RF, Wandell BA (2013) Human trichromacy revisited. *Proc Natl Acad Sci USA* 110:E260–E269.
10. Do MTH, et al. (2009) Photon capture and signalling by melanopsin retinal ganglion cells. *Nature* 457:281–287.
11. Brown TM, et al. (2010) Melanopsin contributions to irradiance coding in the thalamo-cortical visual system. *PLoS Biol* 8:e1000558.
12. Allen AE, et al. (2014) Melanopsin-driven light adaptation in mouse vision. *Curr Biol* 24:2481–2490.
13. Davis KE, Eleftheriou CG, Allen AE, Procyk CA, Lucas RJ (2015) Melanopsin-derived visual responses under light adapted conditions in the mouse dLGN. *PLoS One* 10:e0123424.
14. Spitschan M, Datta R, Stern AM, Brainard DH, Aguirre GK (2016) Human visual cortex responses to rapid cone and melanopsin-directed flicker. *J Neurosci* 36:1471–1482.
15. Spitschan M, Jain S, Brainard DH, Aguirre GK (2014) Opponent melanopsin and S-cone signals in the human pupillary light response. *Proc Natl Acad Sci USA* 111:15568–15572.
16. Benson NC, Butt OH, Brainard DH, Aguirre GK (2014) Correction of distortion in flattened representations of the cortical surface allows prediction of V1-V3 functional organization from anatomy. *PLoS Comput Biol* 10:e1003538.
17. Spitschan M, Aguirre GK, Brainard DH (2015) Selective stimulation of penumbral cones reveals perception in the shadow of retinal blood vessels. *PLoS One* 10:e0124328.
18. Asano Y, Fairchild MD, Blondé L (2016) Individual colorimetric observer model. *PloS one* 11:e0145671.
19. Zaidi FH, et al. (2007) Short-wavelength light sensitivity of circadian, pupillary, and visual awareness in humans lacking an outer retina. *Curr Biol* 17:2122–2128.
20. Schmidt TM, Chen SK, Hattar S (2011) Intrinsically photosensitive retinal ganglion cells: Many subtypes, diverse functions. *Trends Neurosci* 34:572–580.
21. Winawer J, Witthoft N (2015) Human V4 and ventral occipital retinotopic maps. *Vis Neurosci* 32:E020.
22. Allen AE, Storchi R, Martial FP, Bedford R, Lucas RJ (2017) Melanopsin contributions to the representation of images in the early visual system. *Curr Biol* 27:1623–1632.
23. Liao HW, et al. (2016) Melanopsin-expressing ganglion cells on macaque and human retinas form two morphologically distinct populations. *J Comp Neurol* 524:2845–2872.
24. Joo HR, Peterson BB, Dacey DM, Hattar S, Chen SK (2013) Recurrent axon collaterals of intrinsically photosensitive retinal ganglion cells. *Vis Neurosci* 30:175–182.